Research Square

Preprints are preliminary reports that have not undergone peer review.
They should not be considered conclusive, used to inform clinical practice,
or referenced by the media as validated information.

Unconventional Endocytic Pathways and Receptor Plasticity Support FMDV Internalization and Replication in Porcine Mesenchymal Stromal Cells

Cristina Pérez-García
National Institute for Agricultural and Food Research and Technology, Spanish National Research Council (INIA-CSIC)

Alexandra Calle
National Institute for Agricultural and Food Research and Technology, Spanish National Research Council (INIA-CSIC)

Elisa Torres
National Institute for Agricultural and Food Research and Technology, Spanish National Research Council (INIA-CSIC)

Esther Blanco
National Institute for Agricultural and Food Research and Technology, Spanish National Research Council (INIA-CSIC)

Miguel Ángel Ramírez
ma.ramirez@csic.es

National Institute for Agricultural and Food Research and Technology, Spanish National Research Council (INIA-CSIC)

Article

Keywords: Foot-and-mouth disease virus, porcine mesenchymal stromal cells, integrin β6, caveolae-mediated endocytosis, non-canonical entry, membrane trafficking

Posted Date: October 21st, 2026

DOI: https://doi.org/10.21203/rs.3.rs-10986674/v1

License: This work is licensed under a Creative Commons Attribution 4.0 International License.
Read Full License

Additional Declarations: No competing interests reported.

Abstract

Foot-and-Mouth Disease Virus (FMDV) infection is defined by canonical receptor uptake in epithelial cells, but its entry mechanisms in non-epithelial stromal cells remain poorly understood. We investigated FMDV infection dynamics, receptor profiling, and endocytic pathways in Iberian pig MSCs from abdominal adipose, subcutaneous adipose, dermal skin, and peripheral blood, using isolates A/IRN/1/2005 (A-IRN) and O/IRN/8/2005 (O-IRN) alongside BHK-21 and PK-15 epithelial controls. Both serotypes induced dose-dependent cytopathic effects in MSCs by 48 h post-infection and supported productive viral replication. Abdominal adipose and peripheral blood MSCs showed the highest A-IRN replication, whereas abdominal and subcutaneous adipose MSCs were most permissive for O-IRN. Flow cytometry revealed a unique MSC receptor profile: exclusive β_6 integrin expression, variable $\alpha_v\beta_6$, restricted $\alpha_v\beta_3$ in blood MSCs, uniform JMJD6 expression, and absence of heparan sulfate proteoglycans. Pharmacological inhibition assays showed serotype-dependent entry in MSCs: A-IRN required actin dynamics and tyrosine kinases, whereas O-IRN internalization was selectively sensitive to genistein, a caveolae inhibitor. Surprisingly, blocking clathrin endocytosis enhanced A-IRN replication in BHK-21 cells, suggesting viral uptake redirection. These findings demonstrate that porcine MSCs are permissive FMDV targets using non-canonical, serotype-specific endocytic pathways and distinct receptors.

Introduction

Foot-and-Mouth Disease Virus (FMDV; genus Aphthovirus) is classically recognized for its marked epithelial tropism, where viral entry is mediated by canonical α_v integrin heterodimers, primarily $\alpha_v\beta_6$ and $\alpha_v\beta_3$, and internalization proceeds predominantly through clathrin-mediated endocytosis [1, 2]. Viral replication initiates in the oropharyngeal and nasal mucosa, establishing local infection before systemic dissemination. Early infection stages are accompanied by marked alterations in host immune signaling, including suppression of pro-inflammatory cytokines (IL-1β, IL-6, TNFα) and induction of the immunoregulatory cytokine IL-10 [1]. Such modulation of cytokine networks creates an anti-inflammatory environment that may facilitate early viral evasion and prolonged replication cycles within lymphatic and stromal tissues before clinical clearance. This immunosuppressive context raises the possibility that mesenchymal stromal cells (MSCs), known for their immune regulatory and reparative capacities, could act as supportive host niches for FMDV infection.

MSCs are multipotent stromal cells capable of modulating innate and adaptive immune responses during inflammation [2, 3]. Upon activation by cytokines such as TNF-α and IFN-γ, MSCs polarize toward the MSC2 phenotype, characterized by enhanced anti-inflammatory and tissue-reparative functions [4, 5]. This transition involves AhR-dependent interactions with innate lymphoid cells that promote epithelial regeneration via amphiregulin [6], alongside the induction of tolerogenic dendritic cells through the IL-10, PGE2, galectin-3, and IDO pathways [7]. These properties place MSCs at the intersection of viral immune evasion, tissue homeostasis, and repair, which are key processes exploited by persistent pathogens.

In this study, we utilized a well-characterized primary Iberian pig MSC platform to elucidate the cellular and molecular mechanisms governing FMDV entry and replication in non-epithelial stromal cells. Specifically, we investigated: (i) the cell-surface landscape and distribution of canonical ($\alpha_v\beta_6$, $\alpha_v\beta_3$, heparan sulfate) and alternative (JMJD6, isolated β_6) receptors across porcine MSCs derived from four distinct anatomical origins (abdominal adipose, subcutaneous adipose, dermal skin, and peripheral blood); (ii) the selective reliance on clathrin-, caveolae-, actin-, and tyrosine kinase-dependent endocytic pathways using specific pharmacological inhibitors; and (iii) the mechanistic links between receptor availability, endocytic redirection, and viral permissiveness using field isolates A/IRN/1/2005 and O/IRN/8/2005 alongside BHK-21 and PK-15 epithelial controls. By defining these entry dynamics, we demonstrate that primary porcine MSCs serve as permissive stromal targets for FMDV through non-canonical, serotype-specific endocytic pathways, highlighting the remarkable plasticity of membrane trafficking machinery in primary progenitor cells.

Results

Porcine MSCs are permissive to FMDV infection in a serotype-specific manner

To assess the susceptibility of porcine MSCs to FMDV, Iberian pig MSCs previously established and characterized by our group [8] were infected with FMDV isolates of serotypes A-IRN and O-IRN. Established epithelial cell lines known to efficiently support FMDV replication (BHK-21 and PK-15) were used as reference controls [16, 17]. Both viral serotypes induced clear, dose-dependent cytopathic effects in MSCs, characterized by cell rounding, detachment, and cytoplasmic vacuolization, which became evident 48 h post-infection (hpi) at both low (0.1 PFU/cell) and high (1 PFU/cell) multiplicities of infection (Fig. 1).

Remarkably, porcine MSCs supported productive infection and viral replication dynamics comparable to those observed in conventional permissive cell lines, highlighting their unexpected competence as FMDV-target cells. These findings prompted detailed temporal and mechanistic analyses to further characterize the pathways of FMDV replication and entry pathways in this stromal cell population.

Porcine MSC Permissiveness to FMDV is Shaped by Host Cell Subtype and Influenced by Serotype-Specific Tropism.

Temporal analysis of FMDV replication revealed marked differences associated with host cell type but not with viral serotype. RT-qPCR quantification showed that porcine MSCs efficiently supported replication of both A-IRN (Fig. 2) and O-IRN (Fig. 3) strains, with substantially lower C_t values than PK-15 cells in infections with A-IRN, indicating higher viral RNA levels. Among the tested cell lines, BHK-21 cells exhibited the most rapid and sustained decrease in C_t values for both serotypes, consistent with their high permissiveness. Among the MSC populations, AA-MSCs and PB-MSCs showed the lowest C_t values

at 23 h post-infection (hpi) with A-IRN, whereas AA-MSCs and SCA-MSCs displayed the lowest C_t values at 23 hpi with O-IRN. Collectively, these results indicate that FMDV replication dynamics are strongly influenced by host cell identity, with porcine MSCs displaying selective permissiveness that supports efficient FMDV RNA replication in vitro.

MSC receptor profiling identifies alternative entry determinants.

Flow cytometric analysis of the four porcine MSC lines revealed receptor expression profiles distinct from those of the epithelial PK-15 controls. While all cell types expressed β_1 integrin, MSCs displayed several distinguishing patterns.

- β_6 integrin was exclusively expressed in MSCs and was absent in PK-15 cells.
- $\alpha_v\beta_6$ integrin showed variable expression across MSC lines but was undetectable in AA-MSCs.
- $\alpha_v\beta_3$ integrin was restricted to PB-MSCs and PK-15 cells (Fig. 4).
- BHK-21 cells were negative for all integrins under these experimental conditions (Fig. 4).
- JMJD6 was uniformly expressed in MSCs, whereas heparan sulfate proteoglycans were undetectable (Fig. 5).

This MSC-specific receptor landscape suggests that FMDV entry may rely on non-canonical uptake pathways, including β_6 integrin–mediated internalization and JMJD6-dependent mechanisms, potentially compensating for the absence of heparan sulfate binding. These receptor characteristics likely contribute to the selective susceptibility of MSCs to specific FMDV serotypes in the host.

Distinct endocytic pathways mediate serotype-specific MSC infections.

Pharmacological inhibition of viral entry revealed divergent endocytic requirements for A-IRN and O-IRN infections in porcine MSCs. Treatment with genistein and jasplakinolide significantly reduced A-IRN replication in AA-MSCs and SCA-MSCs, implicating caveolae-dependent endocytosis and actin cytoskeleton dynamics in viral entry (Fig. 6). In contrast, O-IRN infection was selectively sensitive to genistein inhibition, with the most pronounced reductions observed in SCA-MSCs and PK-15 cells (Fig. 7).

Unexpectedly, chlorpromazine treatment, which disrupts clathrin-mediated endocytosis, enhanced A-IRN infection in BHK-21 cells, suggesting that inhibition of clathrin-coated pit formation may divert virions toward alternative, highly productive internalization routes in this line. Conversely, methyl-β-cyclodextrin (MβCD) treatment, which disrupts lipid rafts through membrane cholesterol depletion, exerted no significant inhibitory effect on viral replication in any of the tested cell lines for either serotype.

Together, these findings demonstrate that FMDV utilizes distinct, serotype-dependent endocytic mechanisms across different host cell populations, underscoring the molecular complexity of its cell-entry adaptation strategies.

Discussion

Our results demonstrate that porcine mesenchymal stromal cells are permissive to FMDV infection in a serotype- and cell type-specific manner, revealing an unexpected host tropism in this stromal population.

Iberian pig MSCs supported productive infection with both A/IRN/1/2005 and O/IRN/8/2005, exhibiting cytopathic effects and replication kinetics comparable to those observed in the highly permissive BHK-21 control epithelial cell line. Notably, in the case of the A/IRN/1/2005 isolate, MSCs demonstrated enhanced replication efficiency and more pronounced CPE than the porcine epithelial cell line PK-15, which showed lower susceptibility to this serotype. Among MSCs, AA-MSCs and PB-MSCs showed the lowest C_t values for A-IRN at 23 hpi, indicating the highest levels of viral RNA accumulation, whereas AA-MSCs and SCA-MSCs exhibited the lowest C_t values for O-IRN, identifying them as the most permissive populations for this serotype. These patterns indicate that host cell identity and viral serotype function in concert to shape replication kinetics across MSC subsets. As expected, BHK-21 cells consistently reached the lowest and most rapidly decreasing C_t values for both serotypes, confirming their high permissiveness and efficient support of FMDV replication.

Flow cytometric profiling revealed that MSCs exhibited a distinct receptor landscape, including exclusive β_6 integrin expression, variable $\alpha_v\beta_6$, PB-MSC–restricted $\alpha_v\beta_3$, and uniform JMJD6 expression, whereas heparan sulfate was undetectable. These observations suggest that FMDV entry into MSCs relies on non-canonical pathways, potentially mediated by β_6 integrin and JMJD6, compensating for the absence of classical heparan sulfate–dependent uptake [18]. This is particularly noteworthy as efficient infection of conventional cell lines in culture, such as BHK-21, has been shown to critically require initial binding to the cell surface heparan sulfate[19] [20].

Pharmacological inhibition further demonstrated the serotype-dependent endocytic requirements. Treatment with jasplakinolide (an actin-stabilizing agent) and genistein (a tyrosine kinase inhibitor) significantly reduced FMDV entry and replication in porcine mesenchymal stromal cell lines (AA-MSC and SCA-MSC) infected with the A-IRN serotype. In contrast, during O-IRN infection, inhibition was observed only with genistein in SCA-MSC and PK-15 cells. These findings indicate that the mechanism of viral internalization differs according to viral serotype and host cell type. The inhibitory effect of jasplakinolide suggests that actin cytoskeleton dynamics, rather than the mere presence of filamentous actin, are required for A-IRN entry into MSCs, consistent with previous studies showing that actin stabilization interferes with endocytic processes [21].

Conversely, the inhibitory effect of genistein aligns with its role as a blocker of caveolae-mediated endocytosis through the inhibition of tyrosine kinase–dependent phosphorylation events [22, 23]. The observation that porcine MSCs lack heparan sulfate proteoglycans but remain permissive to FMDV infection suggests that viral entry proceeds through alternative, non-canonical pathways. The inhibition of A-IRN infection by genistein, a tyrosine kinase inhibitor that disrupts caveolae/lipid raft–mediated endocytosis, strongly supports a mechanism involving caveolin-dependent internalization rather than

clathrin-mediated uptake. Notably, several non-enveloped viruses exploit caveolae for cell entry in the absence of heparan sulfate binding and rely on proteinaceous or glycosphingolipid receptors. For example, Simian virus 40 enters via caveolin-1–positive vesicles through interaction with GM1 ganglioside [24], while Echovirus 1 uses $\alpha_2\beta_1$ integrin to internalize through a cholesterol- and dynamin-dependent caveolar route [25]. Similarly, Coxsackievirus A9 engages $\alpha_v\beta_6$ integrin and enters through a genistein-sensitive pathway that is independent of heparan sulfate [26].

Consistent with these precedents, our receptor profiling revealed that porcine MSCs express β_6 integrin and variably express $\alpha_v\beta_6$, both of which are recognized as FMDV receptors capable of mediating infection through lipid raft–associated endocytosis [11, 27]. Previous studies have demonstrated that integrin-mediated FMDV entry can proceed through caveolar or clathrin-independent routes, depending on the host cell context, whereas cell culture–adapted strains that acquire heparan sulfate binding shift toward clathrin-mediated endocytosis [28]. The MSC phenotype described here, heparan sulfate–negative yet genistein-sensitive, therefore, aligns with the integrin-dependent, caveola-associated entry model characteristic of field FMDV isolates. These findings underscore the ability of FMDV to flexibly utilize distinct endocytic routes across host cell types, reflecting the adaptive plasticity in receptor usage and internalization mechanisms.

As previously reported, BHK-21 cells were negative for all integrins analyzed, consistent with the notion that viral infection in this cell line occurs through non–integrin-dependent mechanisms [20, 29]. Interestingly, treatment of BHK-21 cells with chlorpromazine, a classical inhibitor of clathrin-mediated endocytosis, significantly increased A-IRN viral infection. This paradoxical enhancement suggests that FMDV entry into BHK-21 cells is not primarily clathrin-dependent and that inhibition of this pathway may redirect viral uptake toward more permissive entry routes, possibly involving caveolae or macropinocytosis. Similar observations have been reported for other picornaviruses, including coxsackievirus B3 and echovirus 1, where chlorpromazine treatment enhances viral infection by altering endocytic trafficking and promoting alternative internalization pathways [30, 31].

Together, these results support the notion that FMDV entry in porcine MSCs is governed by the interplay between cytoskeletal dynamics and kinase signaling rather than canonical receptor-mediated uptake, and that the choice of entry route can vary between cell types, such as MSCs and BHK-21. These findings underscore the importance of considering both viral serotype and host cell phenotype when designing antiviral strategies that target viral entry mechanisms. Taken together, our findings reveal a multi-layered host-pathogen interaction: while the primary endocytic route (caveolae- vs. actin-dependent mechanisms) is strictly dictated by the viral serotype (A-IRN vs. O-IRN), overall replication efficiency and cellular permissiveness are shaped by the specific MSC lineage. This demonstrates that FMDV entry and replication in non-epithelial stromal niches are not mutually exclusive or uniformly regulated, but instead rely on serotype-specific adaptations to distinct MSC receptor profiles and endocytic environments.

Identifying MSCs as a permissive host population with unconventional viral uptake mechanisms provides critical insights into the mechanisms of viral dissemination and pathogenesis. Stromal niches

may act as localized replication foci, influencing the systemic spread of the virus and modulating host immune responses in vivo [32]. Early FMDV infection in these populations appears to suppress pro-inflammatory cytokines (IL-1β, IL-6, TNF-α) while inducing immunoregulatory mediators such as IL-10 [1]. This creates a transient anti-inflammatory environment that may facilitate early viral evasion and prolonged replication cycles within lymphatic and stromal tissues before clinical clearance.

MSCs, with their high plasticity and immunoregulatory capacity, can polarize toward an MSC2 phenotype under TNF-α and IFN-γ stimulation, acquiring anti-inflammatory and tissue-reparative functions [4, 5]. Furthermore, MSC activation may involve AhR-dependent crosstalk with innate lymphoid cells, promoting epithelial regeneration via amphiregulin and inducing tolerogenic dendritic cells through IL-10, PGE_2, galectin-3, and IDO [7].

Collectively, these findings highlight MSCs as critical mediators at the intersection of viral entry, immune modulation, and tissue repair, revealing novel mechanistic determinants of FMDV host adaptation. Future studies should explore MSC contributions to viral persistence, dissemination, and immune regulation using in vivo infection models, single-cell transcriptomics, and spatial tissue analyses to define their dynamics and fate during natural outbreaks. Such investigations may inform antiviral strategies targeting cell-specific viral entry and persistence mechanisms, thereby improving the control of FMDV infections.

Methods

Cells and viruses

Iberian pig MSC lines derived from distinct tissue sources, including subcutaneous adipose (SCA-MSCs), abdominal adipose (AA-MSCs), dermal skin (DS-MSCs), and peripheral blood (PB-MSCs), were established and characterized as previously described [8].MSCs were used between passages 40 and 50. Additionally, BHK-21 (Baby Hamster Kidney) and porcine kidney epithelial lines (IBRS-2 and PK-15) were obtained from the Centro de Investigación en Sanidad Animal (CISA, INIA-CSIC, Valdeolmos, Spain) and used between passages 30 and 40. These cell lines were used for viral propagation, susceptibility assays, and as experimental controls.

All cell lines were maintained in Dulbecco's Modified Eagle's Medium Low Glucose (DMEM-LG; Hyclone Laboratories, UT, USA) supplemented with 2% non-essential amino acids and antibiotics (100 U/mL penicillin and 100 µg/mL streptomycin). Fetal bovine serum (FCS; Gibco, Australia) was added at 15% for MSCs and 3% for BHK-21 and PK-15 cells. The cultures were incubated at 37°C in a humidified atmosphere with 5% CO2.

FMDV isolates A/IRN/1/2005 (GenBank accession EF208769) and O/IRN/8/2005 (GenBank accession KY091281) were kindly provided by The Pirbright Institute (United Kingdom). Serotype A was propagated in BHK-21 cells and serotype O was propagated in IBRS-2 cells. Third-passage viral stocks were used in

all subsequent experiments. All work involving infectious FMDV was performed in high-containment BSL-3 facilities at CISA.

Viral titers were determined in 96-well microplates and calculated as the 50% tissue culture infectious dose (TCID50) per milliliter using the Reed–Muench method. The serotype O isolate was titrated in IBRS-2 cells, whereas the serotype A isolate was titrated in BHK-21 cells.

RNA Extraction and Quantitative RT-PCR

Total viral RNA was extracted from 50 µL of infected cell culture supernatant using the IndiSpin Pathogen Kit (Indical Biosciences, Leipzig, Germany) following the manufacturer's protocol. RNA concentration and purity were assessed using a NanoDrop ND-1000 spectrophotometer (Thermo Fisher Scientific).

FMDV RNA was quantified by RT-qPCR using serotype-specific assays targeting the VP1-coding regions of Middle Eastern O and A isolates, as previously described [9]. One-step RT-qPCR reactions were performed using the Luna Universal Probe One-Step RT-qPCR Kit (New England Biolabs, Werfen, España). Each 20 µL reaction mixture contained 300 ng of total RNA (in a 5 µL template volume) and 10 µM serotype-specific primer-probe sets.

Amplification was conducted in a LightCycler 96 Real-Time PCR System (Roche Diagnostics, Mannheim, Germany) under the following cycling conditions: reverse transcription at 55°C for 10 min, initial denaturation at 95°C for 1 min, followed by 40 cycles of denaturation at 95°C for 10 s and combined annealing/extension at 58°C for 1 min. The data were analyzed using the LightCycler 96 software under default settings. The results were expressed as cycle threshold (C_t) values, with $C_t < 40$ defined as the limit of detection for positive viral RNA amplification.

Susceptibility Analysis of Porcine MSCs

Subconfluent monolayers of the four MSC lines (AA-MSCs, DS-MSCs, SCA-MSCs, and PB-MSCs) and control cell lines (BHK-21 and PK-15) were prepared by seeding in 6-well plates 48 h prior to infection. Cells were then infected in duplicate with FMDV isolates A/IRN/1/2005 or O/IRN/8/2005 at multiplicities of infection (MOI) of 0.1 and 1 TCID50/cell. Following a 1-hour adsorption period at 37°C, the inoculum was removed, and the monolayers were washed and maintained in the corresponding growth medium. The cultures were monitored for the development of cytopathic effects (CPE) at 24-hour intervals over a 72-hour period.

Kinetics of FMDV Replication

Four MSC lines (AA-MSC, DS-MSC, SCA-MSC and PB-MSC) and control cells (BHK-21 and PK-15) were seeded in 48-well plates 48 h prior to infection. Monolayers were infected in duplicate with each FMDV

serotype at an MOI of 1 in a 200 µL volume. After a 1-hour adsorption period at 37°C, the inoculum was removed to eliminate unbound virions. The cultures were then cultured with 500 µL maintenance medium (DMEM-LG supplemented with 2% FBS).

Samples consisting of both culture supernatants and cell lysates were collected at 2, 4, 6, 8, 14, 17, 20, and 23 hours post-infection (hpi). To release intracellular viruses, the plates were subjected to three freeze-thaw cycles at -70°C and 37°C. Mock-infected controls were processed in parallel under the same conditions. Viral genomic RNA was quantified using RT-qPCR as described above. All data are presented as the mean ± standard deviation (SD) of triplicate reactions from three independent experiments.

Flow Cytometry Analysis of FMDV Receptor Expression on Porcine MSC Lines

Cell cultures at 80–90% confluence were detached and fixed with 4% paraformaldehyde for 10 min at room temperature. Immunostaining was performed as described by Calle et al.[10]. Briefly, cells were incubated with a blocking solution (2% BSA and 0.1% saponin in PBS) for 30 min at room temperature. For intracellular targets, the cells were permeabilized in a solution containing 15 mM glycine, 0.1% saponin, 10 mM HEPES, and 0.5% BSA in PBS.

Primary antibody incubation was performed for 1 h at room temperature using the following specificities: anti-integrins $\alpha_v\beta_3$ (clone LM6096), $\alpha_v\beta_6$ (clone 10D5), and β_6 (clone csβ_6) (all from Sigma-Aldrich); anti-CD29/integrin β_1 (clone TS2/16; kindly provided by Dr. María Yáñez, CBMSO, Madrid, Spain); and anti-heparan sulfate (clone A7L6, Bio-Techne/Novus Biologicals). JMJD6 expression was detected using a rat polyclonal antibody (16476-1-AP, Proteintech).

Following primary incubation, the cells were labeled with appropriate F(ab')2-goat anti-mouse, anti-rabbit, or anti-rat IgG (H + L) cross-adsorbed secondary antibodies conjugated to FITC or APC (Invitrogen). Negative controls were prepared by omitting the primary antibody, and isotype controls were included to establish gating strategies and account for the background fluorescence. Samples were analyzed using a BD FACSCanto flow cytometer (BD Biosciences, San Jose, CA, USA). Data processing and analysis were performed using FlowJo software (version Vx.0.7r2, TreeStar, Ashland, OR, USA).

Pharmacological Inhibition of FMDV Entry Pathways in Porcine MSCs

To dissect the entry mechanisms of FMDV, MSCs, and control cell lines were pretreated for 30 min at 37°C with various pharmacological inhibitors in a 200 µL volume. The concentrations used were based on the established literature, except for Chlorpromazine, which was optimized at 0.013 µM to ensure the absence of cytotoxicity while maintaining inhibitory activity. The inhibitors and their specific targets were as follows.

- Chlorpromazine (0.013 μM) was used to inhibit clathrin-coated pit formation [11].
- Genistein (100 μM) was used to block caveolae-mediated uptake [12, 13].
- Methyl-β-cyclodextrin (MβCD) (10 mM) to deplete membrane cholesterol [14, 15].
- Jasplakinolide (0.2 μM) was used to stabilize actin filaments, inhibiting macropinocytosis [14].

Viral adsorption was performed at an MOI of 1 $TCID_{50}$/cell at 4°C for 1 h in the presence of inhibitors, followed by PBS washes to remove unbound virus. Infection was performed at 37°C in 500 μL of maintenance medium (DMEM-LG supplemented with 2% FBS) with continued inhibitor exposure. Viral loads at 24 hpi were measured by RT-qPCR targeting the FMDV VP1. All the conditions were tested in triplicate.

Statistical Analysis

Data are presented as mean ± SD from minimum of three independent experiments. Statistical significance was determined using two-way ANOVA with Fisher's least significance difference post-hoc testing (GraphPad Prism 10). Statistical significance was set at $p < 0.05$.

Declarations

Author contributions (CRediT Taxonomy)

Cristina Pérez-García: Data curation, Formal analysis, Investigation, Visualization, Writing – review & editing; Alexandra Calle: Data curation, Formal analysis, Investigation, Validation, Writing – review & editing; Elisa Torres: Data curation, Formal analysis, Investigation, Writing – review & editing; Esther Blanco: Data curation, Formal analysis, Funding acquisition, Investigation, Resources, Writing – review & editing; and Miguel Ángel Ramírez: Conceptualization, Data curation, Formal analysis, Funding acquisition, Investigation, Methodology, Project administration, Resources, Supervision, Validation, Visualization, Writing – original draft, Writing – review & editing.

Data Availability

The datasets analysed during the current study include the genome sequences of FMDV isolates A/IRN/1/2005 and O/IRN/8/2005, which are publicly available in GenBank under accession numbers EF208769 and KY091281, respectively.

The datasets generated during and/or analysed during the current study are available from the corresponding author on reasonable request.

Funding

This work was supported by grants from the Spanish Ministerio de Ciencia e Innovación / Agencia Estatal de Investigación (PID2022-140925OB-I00 and PID2025-174584OR-I00) and the European Union's Horizon Europe Research and Innovation Programme under the European Partnership on Animal Health and Welfare (EUPAHW, Grant Agreement No. 101136346; and EUPAHW2.0, Grant Agreement No. HORIZON-CL6-2025-02-FARM2FORK-02-101287378).

Disclosure statement

No potential conflict of interest was reported by the author (s).

Ethics declaration

The porcine mesenchymal stromal cell lines used in this study, including subcutaneous adipose tissue-derived MSCs (SCA-MSCs), abdominal adipose tissue-derived MSCs (AA-MSCs), dermal skin-derived MSCs (DS-MSCs), and peripheral blood-derived MSCs (PB-MSCs), were previously established and characterized by Calle et al. [8]. The tissue samples used for the derivation of these cell lines were collected post mortem from an Iberian boar at a commercial slaughterhouse following routine slaughter. Sample collection was conducted with the knowledge and authorization of the slaughterhouse operator and in accordance with the facility's operational and biosecurity requirements. No animals were subjected to experimental procedures, anesthesia, or euthanasia for the purpose of establishing these cell lines or performing the present study. All experimental procedures related to cell isolation and culture were conducted under an Animal Use Protocol approved by the INIA Animal Experimentation Ethics Committee and complied with the basic standards for the protection of animals used for scientific purposes. All methods were carried out in accordance with relevant guidelines and regulations, including Spanish legislation for animal protection (RD1201/2005) and European Union Directive 86/609/EEC regarding the protection of animals used for research. The present study was carried out exclusively using previously established cell lines.

References

1. Medina, G. N. & Diaz San Segundo, F. Virulence and Immune Evasion Strategies of FMDV: Implications for Vaccine Design. *Vaccines (Basel)*. **12**, 1071 (2024).
2. Ayala-Cuellar, A. P., Kang, J. H., Jeung, E. B. & Choi, K. C. Roles of Mesenchymal Stem Cells in Tissue Regeneration and Immunomodulation. *Biomol. Ther. (Seoul)*. **27**, 25–33 (2019).
3. Calle, A. & Ramírez, M. Á. Mesenchymal Stem Cells in Embryo-Maternal Communication under Healthy Conditions or Viral Infections: Lessons from a Bovine Model. *Cells* **11**, 1858 (2022).
4. Sleem, A. & Saleh, F. Mesenchymal stem cells in the fight against viruses: Face to face with the invisible enemy. *Curr. Res. Transl Med.* **68**, 105–110 (2020).

5. Thanunchai, M., Hongeng, S. & Thitithanyanont, A. Mesenchymal Stromal Cells and Viral Infection. *Stem Cells Int* 860950 (2015). (2015).
6. van Hoeven, V. et al. Mesenchymal Stromal Cells Stimulate the Proliferation and IL-22 Production of Group 3 Innate Lymphoid Cells. *J. Immunol.* **201**, 1165–1173 (2018).
7. Volarevic, V. et al. Mesenchymal stem cell-derived factors: Immuno-modulatory effects and therapeutic potential. *Biofactors* **43**, 633–644 (2017).
8. Calle, A. et al. Iberian pig mesenchymal stem/stromal cells from dermal skin, abdominal and subcutaneous adipose tissues, and peripheral blood: in vitro characterization and migratory properties in inflammation. *Stem Cell. Res. Ther.* **9**, 178 (2018).
9. Reid, S. M. et al. Development of tailored real-time RT-PCR assays for the detection and differentiation of serotype O, A and Asia-1 foot-and-mouth disease virus lineages circulating in the Middle East. *J. Virol. Methods*. **207**, 146–153 (2014).
10. Calle, A. et al. Bovine peripheral blood MSCs chemotax towards inflammation and embryo implantation stimuli. *J. Cell. Physiol.* **236**, 1054–1067 (2021).
11. O'Donnell, V., LaRocco, M., Duque, H. & Baxt, B. Analysis of foot-and-mouth disease virus internalization events in cultured cells. *J. Virol.* **79**, 8506–8518 (2005).
12. Chen, S. et al. The endocytosis of foot-and mouth disease virus requires clathrin and caveolin and is dependent on the existence of Rab5 and Rab7 in CHO-677 cells. *Vet. Microbiol.* **274**, 109550 (2022).
13. Zhang, L. et al. Tembusu virus enters BHK-21 cells through a cholesterol-dependent and clathrin-mediated endocytosis pathway. *Microb. Pathog*. **147**, 104242 (2020).
14. Han, S. C. et al. Productive Entry of Foot-and-Mouth Disease Virus via Macropinocytosis Independent of Phosphatidylinositol 3-Kinase. *Sci. Rep.* **6**, 19294 (2016).
15. Anwar, A., Helou, M., Hervol, J. & Levine, A. D. Impact of Caveolin-Mediated Endocytosis on the Trafficking of HIV within the Colonic Barrier. *J. Virol.* **96**, e0020222 (2022).
16. Gao, Y., Yong, F., Yan, M., Wei, Y. & Wu, X. MiR-361 and miR-34a suppress foot-and-mouth disease virus proliferation by activating immune response signaling in PK-15 cells. *Vet. Microbiol.* **280**, 109725 (2023).
17. Yang, J. et al. Profiling and functional analysis of differentially expressed circular RNAs identified in foot-and-mouth disease virus infected PK-15 cells. *Vet. Res.* **53**, 24 (2022).
18. O'Donnell, V., Larocco, M. & Baxt, B. Heparan sulfate-binding foot-and-mouth disease virus enters cells via caveola-mediated endocytosis. *J. Virol.* **82**, 9075–9085 (2008).
19. Jackson, T. et al. Efficient infection of cells in culture by type O foot-and-mouth disease virus requires binding to cell surface heparan sulfate. *J. Virol.* **70**, 5282–5287 (1996).
20. Harvey, Y. et al. An Improved αvβ6-Receptor-Expressing Suspension Cell Line for Foot-and-Mouth Disease Vaccine Production. *Viruses* **14**, 621 (2022).
21. Schafer, D. A., D'Souza-Schorey, C. & Cooper, J. A. Actin assembly at membranes controlled by ARF6. *Traffic* 1, 892–903 (2000).

22. Doherty, G. J. & McMahon, H. T. Mechanisms of endocytosis. *Annu. Rev. Biochem.* **78**, 857–902 (2009).
23. Nabi, I. R. & Le, P. U. Caveolae/raft-dependent endocytosis. *J. Cell. Biol.* **161**, 673–677 (2003).
24. Pelkmans, L., Kartenbeck, J. & Helenius, A. Caveolar endocytosis of simian virus 40 reveals a new two-step vesicular-transport pathway to the ER. *Nat. Cell. Biol.* **3**, 473–483 (2001).
25. Pietiäinen, V. et al. Echovirus 1 endocytosis into caveosomes requires lipid rafts, dynamin II, and signaling events. *Mol. Biol. Cell.* **15**, 4911–4925 (2004).
26. Heikkilä, O. et al. Internalization of coxsackievirus A9 is mediated by {beta}2-microglobulin, dynamin, and Arf6 but not by caveolin-1 or clathrin. *J. Virol.* **84**, 3666–3681 (2010).
27. Jackson, T., Mould, A. P., Sheppard, D. & King, A. M. Integrin alphavbeta1 is a receptor for foot-and-mouth disease virus. *J. Virol.* **76**, 935–941 (2002).
28. Martín-Acebes, M. A., González-Magaldi, M., Sandvig, K., Sobrino, F. & Armas-Portela, R. Productive entry of type C foot-and-mouth disease virus into susceptible cultured cells requires clathrin and is dependent on the presence of plasma membrane cholesterol. *Virology* **369**, 105–118 (2007).
29. Bai, X. W. et al. Engineering Responses to Amino Acid Substitutions in the VP0- and VP3-Coding Regions of PanAsia-1 Strains of Foot-and-Mouth Disease Virus Serotype O. *J Virol* **93**, e02278–e02218 (2019 04 01).
30. Marjomäki, V. et al. Internalization of echovirus 1 in caveolae. *J. Virol.* **76**, 1856–1865 (2002).
31. Mercer, J. & Helenius, A. Virus entry by macropinocytosis. *Nat. Cell. Biol.* **11**, 510–520 (2009).
32. Lebeau, G. et al. Perivascular Mesenchymal Stem/Stromal Cells, an Immune Privileged Niche for Viruses. *Int. J. Mol. Sci.* **23**, 8038 (2022).

Figures

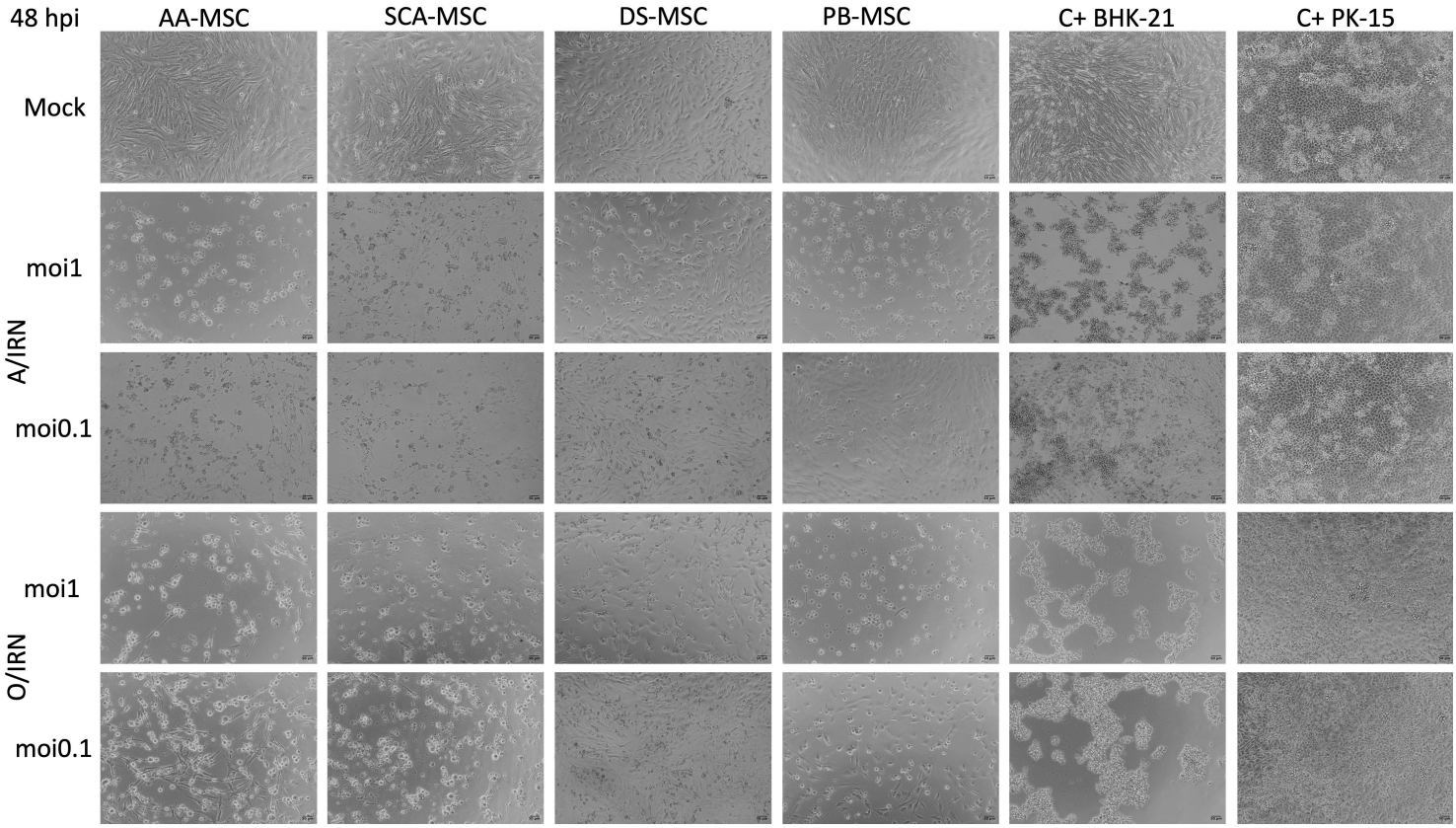
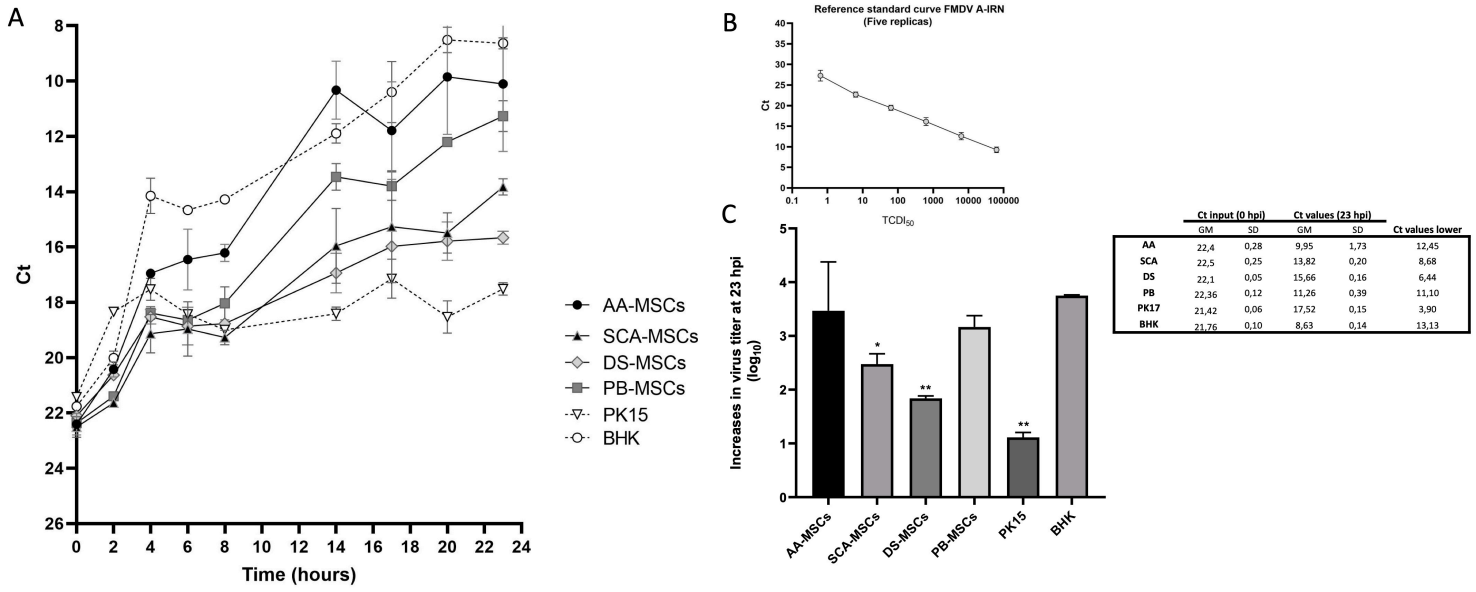


Figure 1

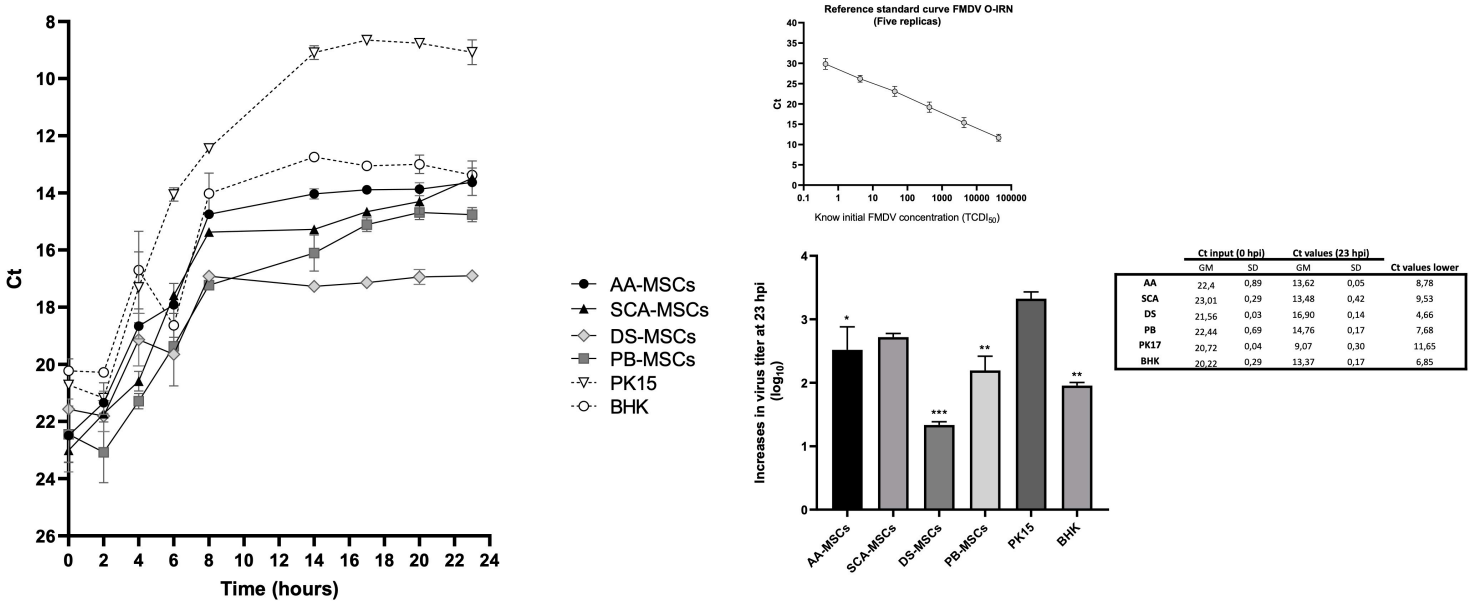
Cytopathic effects in Iberian pig mesenchymal stromal cells (MSCs) following Foot-and-Mouth Disease Virus (FMDV) infection. Phase-contrast micrographs showing uninfected (mock) and MSC monolayers infected with FMDV serotypes A-IRN or O-IRN at multiplicities of infection (MOI) of 0.1 and 1, alongside reference control cell lines (BHK-21 and PK-15) at 48 hpi. Scale bar = 50 µm.



	Ct input (0 hpi)		Ct values (23 hpi)		
	GM	SD	GM	SD	Ct values lower
AA	22,4	0,28	9,95	1,73	12,45
SCA	22,5	0,25	13,82	0,20	8,68
DS	22,1	0,05	15,66	0,16	6,44
PB	22,36	0,12	11,26	0,39	11,10
PK17	21,42	0,06	17,52	0,15	3,90
BHK	21,76	0,10	8,63	0,14	13,13

Figure 2

Replication kinetics, standard curve validation, and quantification of FMDV A-IRN in porcine MSCs. (A) Temporal quantification of FMDV A-IRN genomic RNA. Viral RNA levels were measured using RT-qPCR at multiple time points post-infection (0–23 hpi) across the indicated cell lines to monitor replication kinetics. Uniform initial seeding was confirmed across all lines, with subsequent decreases in C_t values reflecting active viral RNA replication. Data are presented as mean cycle threshold (C_t) ± SD from three independent experiments. (B) Reference standard curve generated by RT-qPCR analysis of known quantities of FMDV A-IRN genome copies. This standard curve demonstrates that a negative shift of 3.5 in C_t values corresponds to a 1.0 $\log_{10}$ increase in viral titer. (C) Quantitative analysis and statistical comparison of FMDV A-IRN replication. The accompanying table summarizes the initial viral input (C_t at 0 hpi), the geometric mean C_t values (±SD) at 0 and 23 hpi, and the net decrease in C_t after 23 hours of infection (final column). This net C_t reduction corresponds directly to the viral titer increases depicted in the bar graph. Statistical significance compared to the reference control cells (BHK-21) is indicated by asterisks (*).



	Ct input (0 hpi)		Ct values (23 hpi)		
	GM	SD	GM	SD	Ct values lower
AA	22,4	0,89	13,62	0,05	8,78
SCA	23,01	0,29	13,48	0,42	9,53
DS	21,56	0,03	16,90	0,14	4,66
PB	22,44	0,69	14,76	0,17	7,68
PK17	20,72	0,04	9,07	0,30	11,65
BHK	20,22	0,29	13,37	0,17	6,85

Figure 3

Replication kinetics, standard curve validation, and quantification of FMDV O-IRN in porcine MSCs. (A) Temporal quantification of FMDV O-IRN genomic RNA. Viral RNA levels were measured using RT-qPCR at multiple time points post-infection (0–23 hpi) across the indicated cell lines to monitor replication kinetics. Uniform initial seeding was confirmed across all lines, with subsequent decreases in C_t values reflecting active viral RNA replication. Data are presented as mean cycle threshold (C_t) ± SD from three independent experiments. (B) Reference standard curve generated by RT-qPCR analysis of known quantities of FMDV O-IRN genome copies, establishing the correlation between C_t shifts and 1.0 $\log_{10}$ changes in viral titer. (C) Quantitative analysis and statistical comparison of FMDV O-IRN replication. The accompanying table summarizes the initial viral input (C_t at 0 hpi), the geometric mean C_t values (±SD)

at 0 and 23 hpi, and the net decrease in C_t after 23 hours of infection (final column), which corresponds to the viral titer increases depicted in the bar graph. Statistical significance compared to the porcine epithelial reference control cells (PK-15) is indicated by asterisks (*).

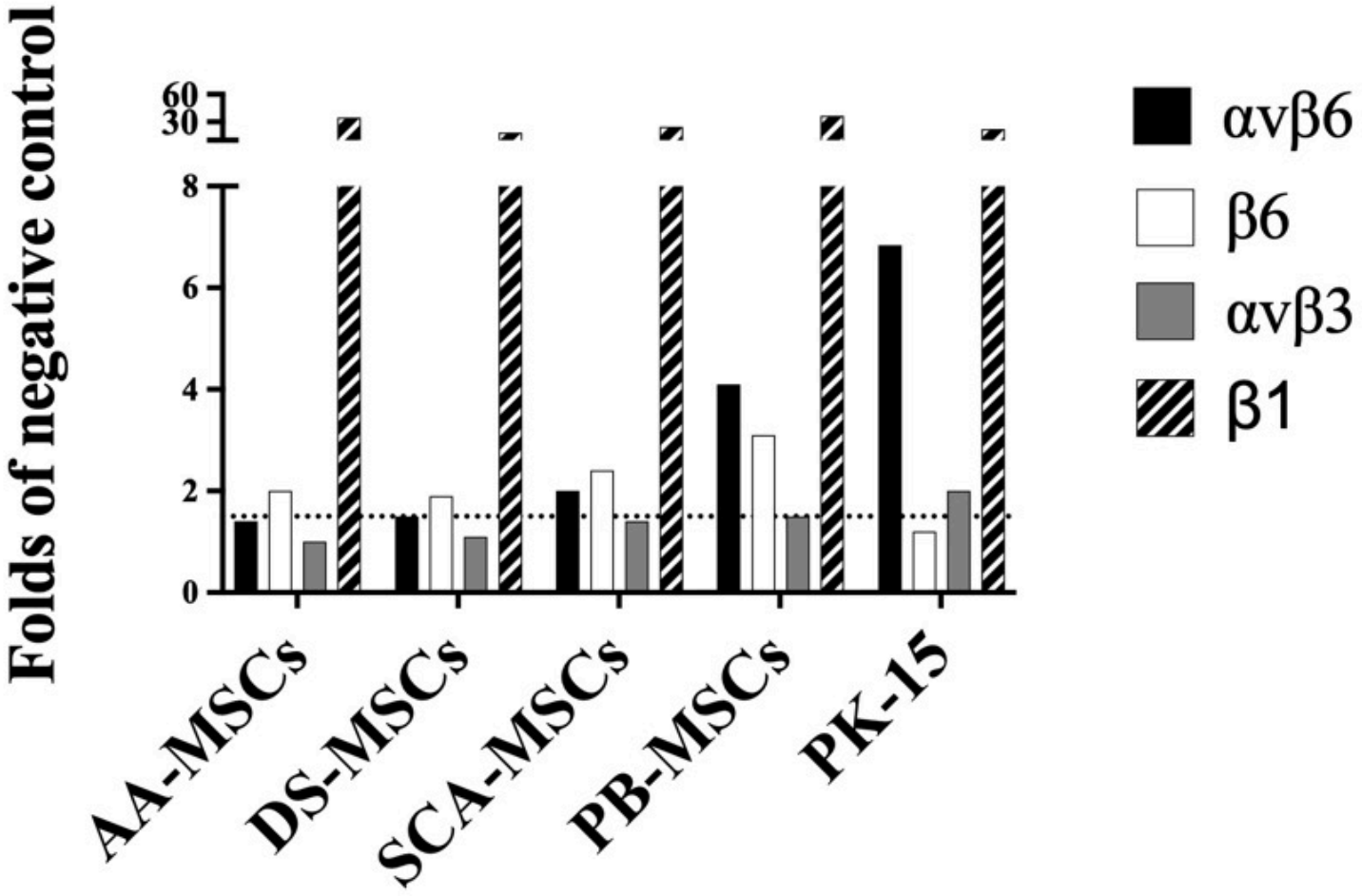


Figure 4

Flow cytometric profiling of FMDV integrin receptors in porcine MSCs and control cell lines. Representative flow cytometry histograms and quantitative analysis of integrins $\alpha_v\beta_3$, $\alpha_v\beta_6$, β_6, and β_1 in four porcine MSC lines (AA-MSCs, DS-MSCs, SCA-MSCs, PB-MSCs), PK-15 epithelial cells, and BHK-21 cells. Distinct receptor expression patterns were observed, characterized by exclusive β_6 integrin detection in MSCs, variable $\alpha_v\beta_6$ expression, $\alpha_v\beta_3$ restriction to PB-MSCs and PK-15 cells, universal β_1 integrin presence and the absence of these integrins in BHK-21 cells.

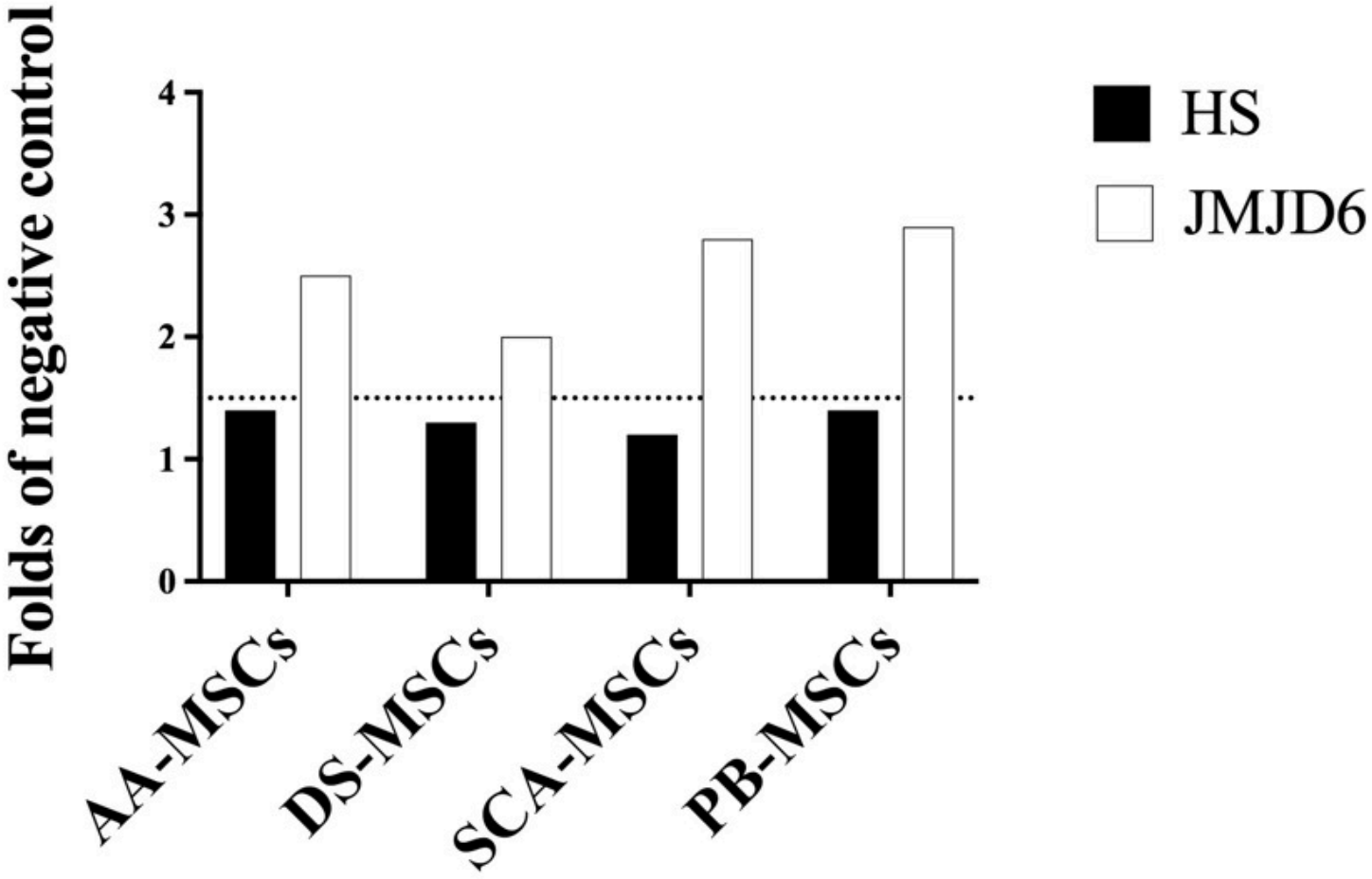


Figure 5

Flow cytometric analysis of heparan sulfate and JMJD6 expression in porcine MSCs. Surface and intracellular expression of JMJD6 and heparan sulfate (HS) proteoglycans evaluated by flow cytometry across porcine MSC lines. All MSC populations displayed uniform expression of JMJD6, whereas HS proteoglycans were below the limit of detection, confirming a receptor profile distinct from that of conventional HS-dependent FMDV-permissive cells.

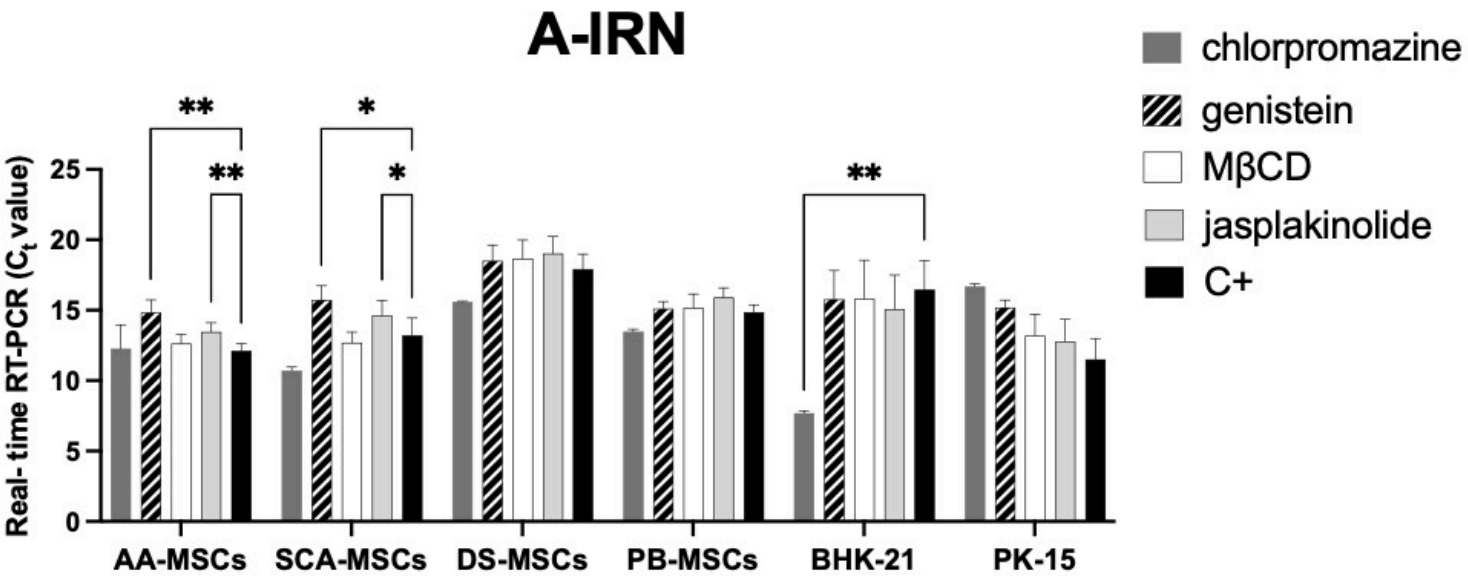


Figure 6

Impact of endocytic pathway inhibitors on FMDV A-IRN replication in porcine MSCs and control cell lines. Cells were pretreated with chlorpromazine (0.013 μM), genistein (100 μM), methyl-β-cyclodextrin (MβCD) (10 mM), or jasplakinolide (0.2 μM) prior to infection with FMDV A-IRN. Viral RNA levels were quantified by RT-qPCR at 24 hpi. Data represent mean ± SD from three independent experiments, highlighting the differential contribution of caveolae/tyrosine kinase activation and actin filament remodeling to A-IRN entry. Statistical significance compared to untreated infected controls is indicated by asterisks ($p < 0.05$).

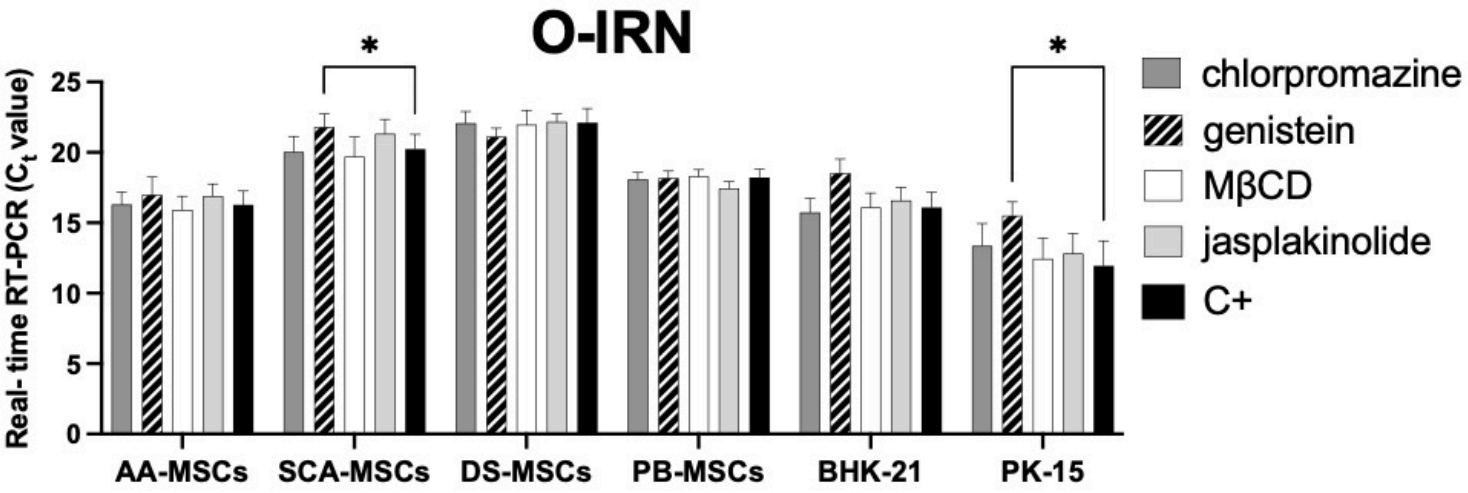


Figure 7

Effect of endocytic pathway inhibitors on FMDV O-IRN replication in porcine MSCs and control cell lines. Cells were pretreated with endocytic inhibitors chlorpromazine (0.013 μM), genistein (100 μM), methyl-β-cyclodextrin (MβCD) (10 mM), or jasplakinolide (0.2 μM) prior to FMDV O-IRN infection, and viral replication was evaluated at 24 hpi by RT-qPCR. Genistein selectively reduced viral replication, exhibiting

the strongest inhibitory effect in SCA-MSCs and PK-15 cells. Data represent mean ± SD from three independent experiments ($p < 0.05$).